

MYELOID NEOPLASIA

Gene expression–based discovery of atovaquone as a STAT3 inhibitor and anticancer agent

Michael Xiang,¹ Haesook Kim,² Vincent T. Ho,^{1,3} Sarah R. Walker,^{1,3} Michal Bar-Natan,¹ Melodi Anahtar,¹ Suhu Liu,¹ Patricia A. Toniolo,¹ Yasmin Kroll,¹ Nichole Jones,¹ Zachary T. Giaccone,¹ Lisa N. Heppler,¹ Darwin Q. Ye,¹ Jason J. Marineau,¹ Daniel Shaw,¹ James E. Bradner,¹ Traci Blonquist,² Donna Neuberg,² Claudio Hetz,^{4,5} Richard M. Stone,^{1,3} Robert J. Soiffer,^{1,3} and David A. Frank^{1,3}

¹Department of Medical Oncology and ²Department of Biostatistics and Computational Biology, Dana-Farber Cancer Institute, Boston, MA; ³Department of Medicine, Brigham and Women's Hospital and Harvard Medical School, Boston, MA; and ⁴Geroscience Center for Brain Health and Metabolism and ⁵Biomedical Neuroscience Institute, Faculty of Medicine, University of Chile, Santiago, Chile

Key Points

- The FDA-approved drug atovaquone is a novel, clinically available inhibitor of STAT3 at standard human plasma concentrations.
- Atovaquone shows anticancer efficacy in vitro, in vivo, and in a retrospective study of AML patient outcomes after atovaquone treatment.

The oncogenic transcription factor signal transducer and activator of transcription 3 (STAT3) is frequently activated inappropriately in a wide range of hematological and solid cancers, but clinically available therapies targeting STAT3 are lacking. Using a computational strategy to identify compounds opposing the gene expression signature of STAT3, we discovered atovaquone (Mepron), an antimicrobial approved by the US Food and Drug Administration, to be a potent STAT3 inhibitor. We show that, at drug concentrations routinely achieved clinically in human plasma, atovaquone inhibits STAT3 phosphorylation, the expression of STAT3 target genes, and the viability of STAT3-dependent hematological cancer cells. These effects were also observed with atovaquone treatment of primary blasts isolated from patients with acute myelogenous leukemia or acute lymphocytic leukemia. Atovaquone is not a kinase inhibitor but instead rapidly and specifically downregulates cell-surface expression of glycoprotein 130, which is required for STAT3 activation in multiple contexts. The administration of oral atovaquone to mice inhibited tumor growth and prolonged survival in a murine model of multiple myeloma. Finally, in patients with acute myelogenous leukemia treated with

hematopoietic stem cell transplantation, extended use of atovaquone for *Pneumocystis* prophylaxis was associated with improved relapse-free survival. These findings establish atovaquone as a novel, clinically accessible STAT3 inhibitor with evidence of anticancer efficacy in both animal models and humans. (*Blood*. 2016;128(14):1845-1853)

Introduction

A crucial component of cancer pathogenesis and progression is the aberrant activation of oncogenic signal transduction pathways. The reliance of neoplastic but not normal cells on such pathways for survival is the basis for targeted cancer therapy.¹ Most research has focused on kinases or other enzymes that are tractable to direct inhibition with small molecules. However, the malignant phenotype is ultimately because of gene expression patterns exerted by the downstream action of transcription factors.

Signal transducer and activator of transcription 3 (STAT3) is a transcription factor that has emerged as a key cancer dependency.^{2,3} STAT3 activation occurs in the cytoplasm by phosphorylation of a critical tyrosine residue, which leads to an activating dimerization. The STAT3 dimer undergoes nuclear translocation, DNA binding, and recruitment of cofactors to mediate the expression of target genes involved in the hallmarks of cancer.⁴ Although STAT3 activation is transient and dispensable in normal cells, it often occurs constitutively in cells of many hematological (and solid) cancers, which depend on

STAT3 for survival.⁵ Thus, targeting inappropriate STAT3 activation is a promising therapeutic strategy and active area of interest.

STAT3 activation in cancer is generally catalyzed by Janus kinases (JAKs). Ruxolitinib, a recently introduced JAK inhibitor, is approved by the US Food and Drug Administration (FDA) for the treatment of primary myelofibrosis, a myeloproliferative neoplasm that is frequently driven by activation of STAT3 or the related transcription factor STAT5.⁶ However, therapies targeting STAT3 for cancer treatment are lacking. Several STAT3 inhibitors have been reported,⁷ but none have received regulatory approval. Therefore, there is a great need for novel STAT3 inhibitors that can be tested in clinical trials. Because STAT3-dependent cancer pathogenesis is primarily the result of STAT3-driven gene expression, we conjectured that novel STAT3 inhibitors could be discovered as compounds that induce opposing gene expression changes.

To test this hypothesis, we used a database of gene expression profiles produced by treating a panel of cell lines with several thousand

Submitted 24 July 2015; accepted 1 August 2016. Prepublished online as *Blood* First Edition paper, 16 August 2016; DOI 10.1182/blood-2015-07-660506.

The online version of this article contains a data supplement.

The publication costs of this article were defrayed in part by page charge payment. Therefore, and solely to indicate this fact, this article is hereby marked "advertisement" in accordance with 18 USC section 1734.

© 2016 by The American Society of Hematology

compounds.⁸ This chemical genomic strategy has succeeded previously in identifying drugs that achieve a specific, desired gene expression end point.^{9,10} Moreover, this gene expression–based approach offered an unbiased means of identifying STAT3 inhibitors acting on any step upstream of target gene transcription. Here, we report the discovery and characterization of atovaquone, an FDA-approved antimicrobial drug not previously known to have any effects in mammalian cells, as a novel, clinically accessible STAT3 inhibitor with evidence of anticancer efficacy in both animal models and humans.

Methods

Connectivity Map analysis

The 12-gene STAT3 signature¹¹ was mapped from murine U74Av2 probes to corresponding human U133A probes. Two genes downregulated by STAT3 activation were similarly mapped. The resulting probe lists (supplemental Table 1, available on the *Blood* Web site) were used to query the Connectivity Map. Detailed results were downloaded, and the “up” score was averaged across all instances for each compound; compounds with fewer than 3 instances were excluded.

Gene expression analysis

Total RNA was harvested using the RNeasy Plus Mini Kit (Qiagen), reverse transcribed using random hexamers, and assayed by quantitative reverse transcription polymerase chain reaction using the indicated primers (supplemental Table 2) as previously described.¹² Gene expression was analyzed in triplicate, normalized by 18S ribosomal RNA, and expressed as mean \pm standard error of the mean.

Cells and tissue culture

Primary leukemia cells, serum, and cells from healthy donors were obtained from the Pasquarello Tissue Bank at the Dana-Farber Cancer Institute (DFCI) under an Institutional Review Board–approved protocol. HEL was a gift of Daniel G. Tenen and grown in RPMI 1640 + 10% fetal bovine serum (FBS). U266 and INA-6 cells were obtained and cultured as previously reported.⁴ Peripheral blood mononuclear cells (PBMCs) were isolated from healthy donors by Ficoll density gradient centrifugation and maintained in RPMI 1640 + 10% FBS. All cells were maintained in a humidified incubator at 37°C with 5% CO₂.

RNA interference

Cells were infected with lentiviral vectors expressing short hairpin RNA targeting a nonmammalian control gene (luciferase) or the indicated targets (supplemental Table 3; Sigma, St. Louis, MO).

Luminometric assays

Luciferase reporter cell lines were described previously.⁴ Firefly luciferase values were normalized by concurrent cell viability. Viable cell number was measured as adenosine triphosphate–dependent luminescence by Cell Titer Glo (Promega).

Flow cytometry

Annexin V/propidium iodide (PI) staining was performed using Apoptosis Detection Kit I (BD Biosciences). Staining for cell-surface receptors was performed in 50 μ L phosphate-buffered saline + 2% FBS with 2 μ L antibody to interleukin-6 (IL-6) receptor (BioLegend #352803) or 5 μ L antibody to glycoprotein 130 (gp130; BD Biosciences #555757) for 20 minutes on ice in the dark. Cells were washed twice, then resuspended in 300 μ L of the same buffer. Intracellular staining of phosphorylated STAT3 was performed on bone marrow samples from acute myeloid leukemia (AML) and acute lymphocytic leukemia (ALL) patients containing at least 90% blasts. Cells were pretreated with atovaquone (25 μ M for 16 hours) or vehicle and then left unstimulated or stimulated with recombinant human IL-6 (50 ng/mL) for 15 minutes at 37°C. Cells were fixed using BD Phosflow Lyse/Fix buffer for 10 minutes and were

then permeabilized in BD Phosflow Perm Buffer III for 30 minutes on ice. Cells were washed in phosphate-buffered saline and stained with anti-pStat3 (pY705) antibody for 1 hour at room temperature. Samples were acquired on a BD FACSCanto II instrument and analyzed with FlowJo software (Treestar).

Animal studies

U266 human multiple myeloma cells were injected in Matrigel subcutaneously in 6- to 8-week-old female NSG mice (Jackson Laboratories, Bar Harbor, ME). Once plasmacytomas had reached a volume of 200 mm³, treatment was begun with vehicle, atovaquone, or Mepron (200 mg/kg per day by gavage). Mepron (GlaxoSmithKline LLC, Research Triangle Park, NC) is a formulation of microfine particles of atovaquone that is used clinically, which also contains the inactive ingredients benzyl alcohol, flavor, poloxamer 188, purified water, saccharin sodium, and xanthan gum. Tumor volume was determined 3 times per week. All studies involving mice were performed according to DFCI Animal Care and Use Committee–approved protocols.

Medical record review

Start and end dates of atovaquone treatment, date of relapse (if applicable), and living status for 232 AML patients who underwent a single allogeneic hematopoietic stem cell transplant (HSCT) at DFCI from 2005 to 2012 were obtained by retrospective chart review with DFCI Institutional Review Board approval. Atovaquone was prescribed as an oral suspension, 750 mg twice daily or 1500 mg once daily.

Western blotting, immunoprecipitation, and antibodies

Western blotting was performed as previously described.¹³ Antibody to phospho-Y705 STAT3 (9131) was from Cell Signaling Technology. Antibodies to total STAT3 (sc-482) and gp130 (sc-656, used at 1:1000) were from Santa Cruz Biotechnology. Phospho-S727 STAT3 antibody was described previously.¹⁴ Antibodies to tubulin (T5168) and β actin (A5316) were from Sigma. All antibodies were used at 1:10 000 dilution for western blot unless otherwise noted.

For immunoprecipitations, cells were lysed in 500 μ L lysis buffer (0.5% NP-40, 150 mM NaCl, 50 mM Tris pH 7.5, with protease and phosphatase inhibitors freshly added at 1:100; Pierce, PI78443) on ice for 15 minutes, then centrifuged for 10 minutes at 14 000 rpm and 4°C. The supernatant was transferred to a new tube and incubated with 10 μ L JAK2 antibody (Santa Cruz sc-278) or a mix of 2 TYK2 antibodies, 10 μ L of each (Santa Cruz sc-5271 and Cell Signaling Technology 9312). Immunoprecipitation was performed overnight at 4°C with rotation. The next day, 75 μ L of protein A/G beads (Santa Cruz sc-2003) were washed twice in lysis buffer, then incubated with immunoprecipitates overnight as before. The next day, the beads were spun down (1 minute at 7500 rpm and 4°C) and washed 3 times with 650 μ L lysis buffer for 10 minutes at 4°C with rotation, then boiled in 50 μ L sample buffer + 10% β -mercaptoethanol. For western blot, 20 μ L was loaded per lane. For detection of pan-phospho-tyrosine, a mixture of 2 pan-phospho-tyrosine antibodies (Cell Signaling Technology 9411 and 9416, 1:1000 of each) was used. Antibody to phospho-Y570 JAK2 was from Millipore (09-241, used at 1:1000).

Drug treatments

For drug treatments, cells were spun down and suspended in fresh media the day prior. Atovaquone (Sigma-Aldrich A7986) was dissolved in dimethyl sulfoxide at a stock concentration of 12.5 mM and used to treat cells at up to 1:500 dilution (up to 0.2% volume-to-volume ratio dimethyl sulfoxide). JAK inhibitor 1 (Millipore 420097) was used at 1 μ M, unless indicated otherwise. Brefeldin A (Millipore 203729) was used at 3 μ g/mL. SC-144 (Tocris, Bristol, United Kingdom) was used at 5 μ M.

Statistical analysis

Survival in a murine cancer model was estimated by comparison of Kaplan-Meier curves using the log-rank test. For AML patients, cumulative incidences of nonrelapse mortality and relapse, with or without death, were analyzed as competing risks. Relapse and nonrelapse mortality were measured from the date of stem cell infusion to disease relapse or death, whichever occurred first. Patients alive without relapse were censored at the time last seen alive. The cumulative

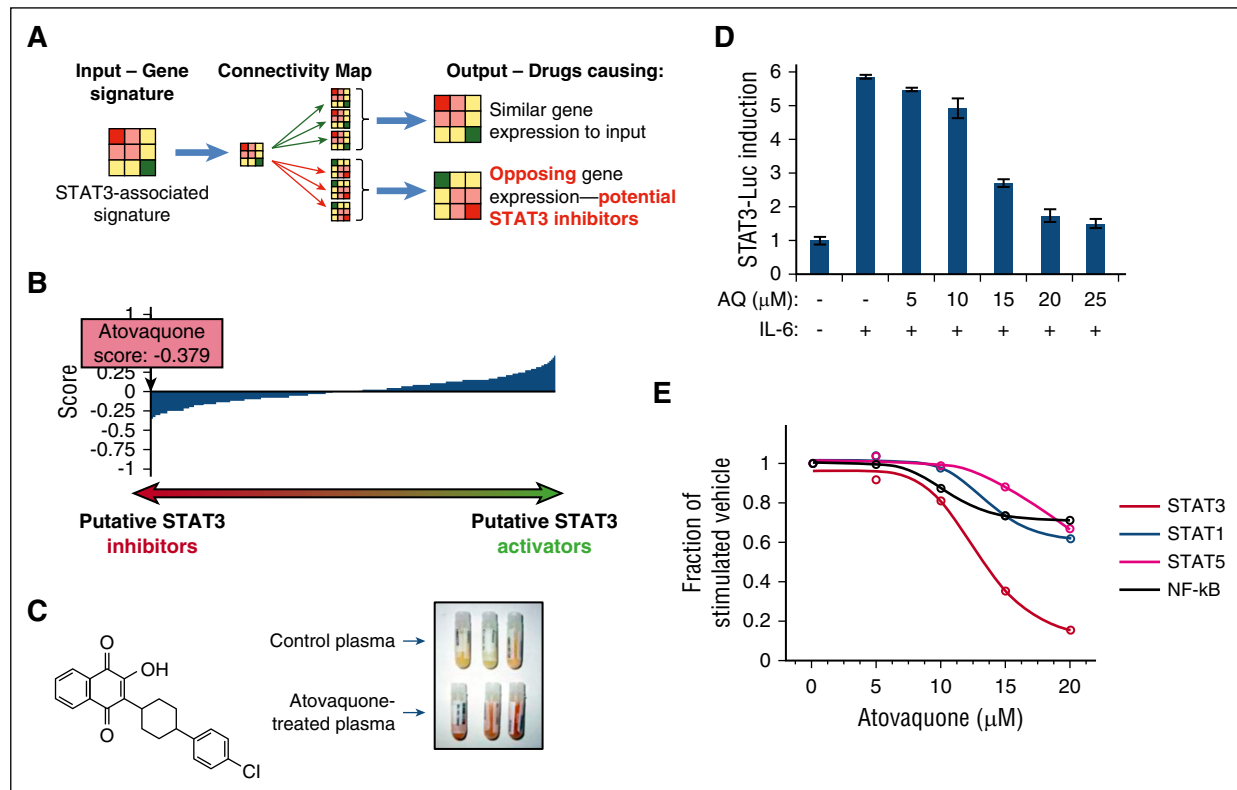


Figure 1. A gene expression-based approach identifies atovaquone as a novel STAT3 inhibitor. (A) Overview of strategy using the Connectivity Map to identify drugs that are potential STAT3 inhibitors based on gene expression. (B) Results from the Connectivity Map analysis. More negative scores indicate more dissimilarity with respect to the STAT3 signature, with atovaquone being the most negatively scoring compound. (C) Chemical structure of atovaquone and appearance of plasma samples isolated from patients taking trimethoprim-sulfamethoxazole (control) or atovaquone. (D) STAT3 reporter cells were pretreated with drug for 1 hour, then stimulated with IL-6 (10 ng/mL) for 5 hours. Activity of firefly luciferase was measured and normalized by viable cell number (Cell Titer Glo). Data are means \pm standard deviation of 2 independent experiments. (E) Effect of atovaquone on STAT3 reporter cells compared with reporter cells for STAT1 (stimulated by interferon- γ), STAT5 (stimulated by prolactin), and NF- κ B (stimulated by tumor necrosis factor α). Data are means from 2 independent experiments.

incidence curves were compared using the Gray test.¹⁵ Competing risks regression analysis was performed using the Fine and Gray model¹⁶ including atovaquone treatment (high vs low exposure), age (≥ 50 vs <50), male patient with female donor, donor type, remission status at conditioning, graft-versus-host disease (GVHD) prophylaxis, patient or donor cytomegalovirus seropositivity, and the occurrence of grade 2 to 4 acute GVHD. Landmark analysis was performed at day 150 after HSCT for all competing risks data analysis. The cutoff of 55 days of atovaquone treatment to separate the patients into “high atovaquone” and “low atovaquone” groups was determined using the restricted cubic spline estimation method for the relationship between the number of days and the change of the log relative hazard of progression-free survival.¹⁷ All testing was 2-sided at the significance level of .05. All calculations were carried out using SAS 9.3 (SAS Institute Inc., Cary, NC) and R version 2.13.2 (the CRAN project).

Results

Atovaquone is a novel, clinically available STAT3 inhibitor

Using a 12-gene signature of STAT3 activation,¹¹ we queried the Connectivity Map⁸ to discover compounds that elicit gene expression changes contrary to the STAT3 signature (Figure 1A). The compound most opposed to the STAT3 signature was atovaquone (Figure 1B), an antimicrobial used to treat or prevent pneumonia caused by the fungal organism *Pneumocystis jirovecii*. It acts by inhibiting *Pneumocystis* respiration and is not known to have any effects on mammalian cells.¹⁸ We focused further studies on atovaquone for several reasons. First,

atovaquone has minimal side effects, and high plasma concentrations (15–30 μ g/mL; 40–80 μ M) are routinely achieved in patients.¹⁸ In fact, atovaquone is a colored compound, and the plasma of patients taking standard doses is visibly imbued with a darker hue (Figure 1C). Furthermore, its FDA-approved status ensures clinical accessibility and greatly reduces the cost and latency of bench-to-bedside translation.

To determine if atovaquone does, in fact, inhibit STAT3 transcriptional function, we first tested it in a cell-based reporter system.⁴ Cells lacking basal STAT3 activity can be treated with the cytokine IL-6 or oncostatin M (OSM) to cause JAK-dependent STAT3 activation and expression of a STAT3-dependent luciferase reporter gene. Using clinically achievable drug concentrations, pretreatment of these cells with atovaquone caused a dose-dependent inhibition of luciferase induction by IL-6 or OSM, indicating suppression of STAT3 transcriptional activity (Figure 1D; supplemental Figure 1A). To determine if atovaquone inhibits STAT3 activity specifically over other transcription factors, we tested it in cell-based reporter systems for STAT1 and STAT5, 2 other STAT family members, and NF- κ B, an unrelated transcription factor. Atovaquone showed specificity for inhibition of STAT3 (Figure 1E). These results demonstrate atovaquone to be a novel, clinically accessible STAT3 inhibitor.

Atovaquone reduces STAT3 phosphorylation, target gene expression, and viability of STAT3-dependent cancer cells

Next, we wished to determine how atovaquone inhibits STAT3 function. Because STAT3 transcriptional activity is critically dependent

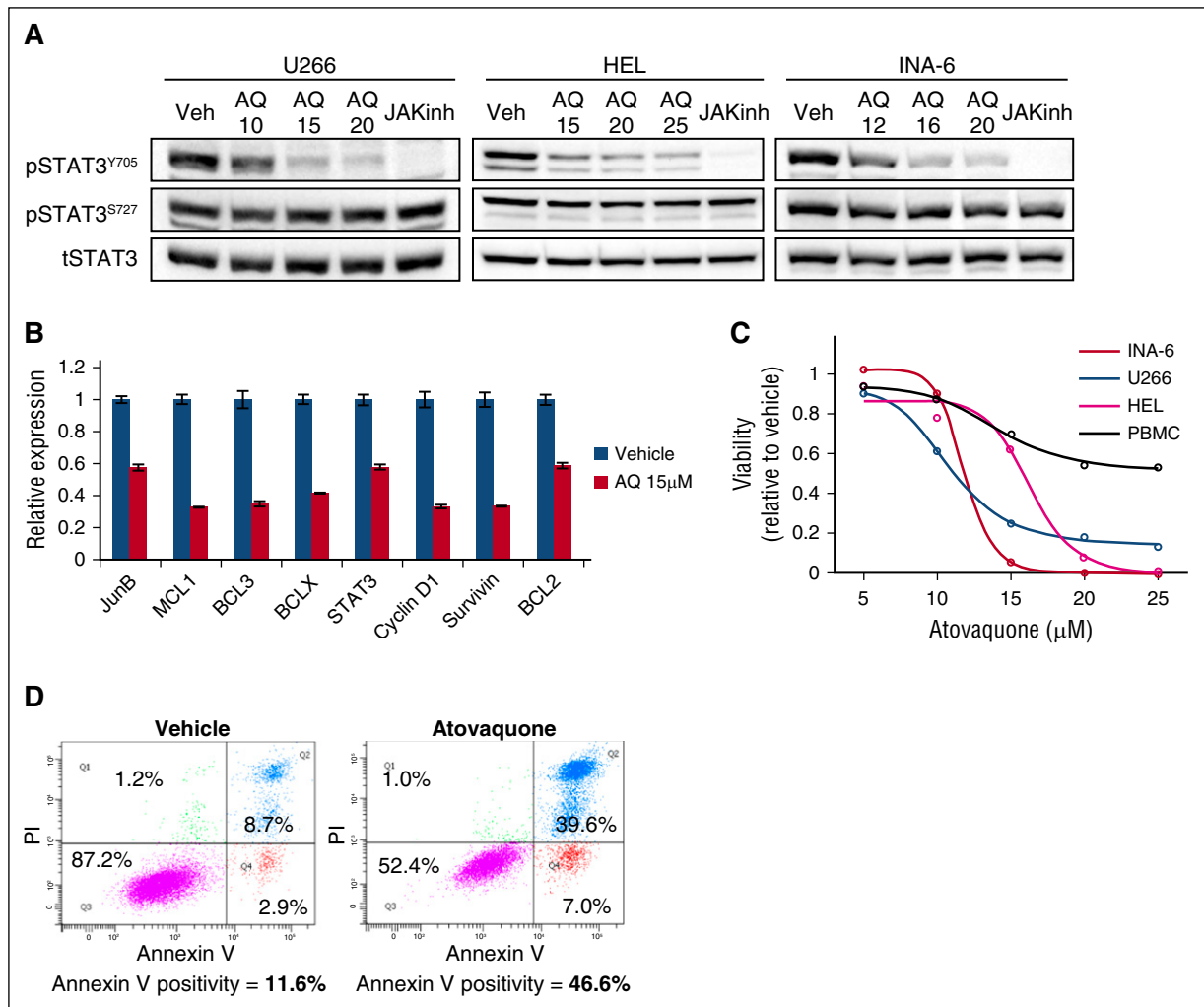


Figure 2. Atovaquone inhibits constitutive STAT3 tyrosine phosphorylation, STAT3 target gene expression, and viability of STAT3-dependent cancer cells through apoptosis. (A) Atovaquone at the indicated concentrations (μM) was used to treat U266 (2.5 hours), HEL (6 hours), or INA-6 cells (4 hours). Treatment with JAK inhibitor 1 (a direct pharmacological JAK inhibitor) at $1 \mu\text{M}$ for the same duration served as a control and comparison. Data are representative of 2 independent experiments. (B) Expression of endogenous STAT3 target genes was assayed by quantitative reverse transcription polymerase chain reaction in U266 cells treated with atovaquone for 6 hours. Data are representative means \pm standard error from 1 of 2 independent experiments. (C) Viable cell number response curve to atovaquone (72-hour treatment) of hematological cancer cells that harbor STAT3 activation, compared with viability of nonmalignant PBMCs (average of 4 donors), which lack STAT3 activation. Data are means from 2 independent experiments. (D) Atovaquone ($15 \mu\text{M}$) treatment of INA-6 cells for 24 hours, followed by staining of cells with annexin V/PI to assay apoptosis. Data are representative of 2 independent experiments.

on tyrosine phosphorylation, we assayed its status by western blot. We found that, in multiple hematological cancer cell lines, atovaquone inhibited constitutive STAT3 tyrosine phosphorylation, whereas STAT3 serine phosphorylation, which is not critical to transcriptional activity, was unaffected (Figure 2A). Furthermore, atovaquone substantially downregulated the expression of multiple endogenous STAT3 target genes in these cellular systems, many of which are crucial to the proliferation and survival of cancer cells, such as *MCL1* and *BCL2* (Figure 2B; supplemental Figure 1B).

We then examined the effect of atovaquone on the viability of STAT3-dependent cancer cells. Survival of the multiple myeloma cell line INA-6 requires constitutive STAT3 activation via supplementation of the culture medium with IL-6.¹⁹ Atovaquone suppressed the viability of INA-6 cells with a 50% inhibitory concentration of $11.9 \mu\text{M}$, with complete loss of viable cells occurring at higher doses (Figure 2C). Other cancer cells with constitutively active STAT3, including U266 (a multiple myeloma cell line with STAT3 activation mediated by autocrine IL-6 production) and HEL (an AML cell line with STAT3

activation mediated by a JAK2-V617F mutation), were also killed by atovaquone at concentrations routinely attained in patients. By contrast, the viability of healthy donor-derived PBMCs, which are nonmalignant and lack STAT3 activation, was preserved. This mirrors the minimal hematological toxicity of atovaquone in vivo.

To ascertain how atovaquone treatment reduced the viability of cancer cells, we performed annexin V and PI staining followed by flow cytometry, which revealed induction of apoptotic cell death (Figure 2D; supplemental Figure 1C).

Atovaquone rapidly and selectively inhibits cell-surface gp130 expression

To investigate how atovaquone inhibits STAT3 phosphorylation, we considered the possibility that atovaquone acts as a JAK inhibitor, because JAKs are responsible for STAT3 activation in these cellular systems. Autophosphorylation of JAK family members was decreased in cells treated with atovaquone, indicating diminished JAK activity

(supplemental Figure 2A-B). However, in vitro kinase assays showed that atovaquone was not a direct JAK inhibitor (supplemental Figure 2C). Therefore, we hypothesized that atovaquone inhibits JAKs indirectly by acting on an upstream signaling component required for JAK activity.

JAK signaling (both wild-type and mutant JAK2-V617F) requires scaffolding interactions with plasma membrane-localized proteins.²⁰ In particular, JAKs are frequently physically associated with the cytoplasmic tail of gp130 (CD130), a transmembrane protein that is necessary for the signaling of IL-6 and OSM, both of which were inhibited by atovaquone (Figure 1D; supplemental Figure 1A). In contrast, gp130 is not involved in the signaling of the cytokines used to activate STAT1, STAT5, and NF- κ B, which were unaffected by atovaquone treatment (Figure 1E). Therefore, we hypothesized that atovaquone inhibits the function or expression of gp130.

We found that atovaquone substantially downregulates the cell-surface expression of gp130 (Figure 3A; supplemental Figure 2D). In contrast, atovaquone had no effect on the cell-surface expression of another protein involved in STAT3 activation, the IL-6 receptor (CD126), suggesting that this is not a general effect on cell-surface proteins. A pharmacological JAK inhibitor did not affect gp130 expression, indicating this effect was not secondary to decreased JAK or STAT3 activity. Lastly, brefeldin A, a compound that inhibits transport of all proteins from endoplasmic reticulum to Golgi, reduced the cell-surface expression of both gp130 and IL-6 receptor, suggesting atovaquone was not inhibiting protein transport in a nonspecific fashion.

Because atovaquone reduced the abundance of gp130 at the cell surface, we asked whether atovaquone concomitantly reduced total gp130 in the cell. To address this question, we performed a time course of atovaquone treatment and measured total cellular gp130 by western blotting. Cell-surface gp130 and STAT3 phosphorylation were both inhibited rapidly, after only 15 minutes (Figure 3B). By contrast, total gp130 was unaffected by atovaquone until at least 60 minutes of treatment, and this late decrease may reflect the degradation of internalized gp130. Thus, atovaquone rapidly and selectively depletes gp130 at the cell surface.

To determine if this depletion of gp130 was sufficient to mediate the signaling and survival effects seen with atovaquone treatment, we took 2 complementary approaches. First, we used short hairpin RNA to deplete gp130 (or STAT3, as a positive control) from INA-6 or U266 cells. Both treatments were sufficient to abrogate phosphorylated STAT3 from these cells, and both led to a decrease in viable cell number associated with increased apoptosis (supplemental Figure 2E-G). Second, we used a small-molecule inhibitor of gp130 function, SC-144.²¹ This compound also led to a prominent decrease in STAT3 phosphorylation and viable cell number (supplemental Figure 2H-I). Thus, the effects of atovaquone on gp130 are sufficient to explain the associated loss of cellular viability.

Atovaquone demonstrates antitumor activity in a murine model of multiple myeloma

Given the efficacy of atovaquone in killing hematological cancer cells at plasma concentrations routinely achieved clinically (Figure 2C), as well as its excellent safety profile in humans, we next wished to assess its activity in an animal model. We used U266 human multiple myeloma cells, which harbor constitutive STAT3 activation from autocrine production of IL-6. Immunodeficient mice were injected with U266 cells to form plasmacytomas, then treated orally with vehicle or atovaquone. We used 2 separate atovaquone treatment groups. The first group was treated with chemically pure atovaquone as in the in vitro

experiments. To ensure the clinical applicability of the study, the second group was treated with brand-name Mepron, the same product administered to patients. The dose of 200 mg/kg per day was selected based on prior reports for murine *Pneumocystis* research²² and corresponds to a dose of 800 to 1500 mg/d in humans,²³ which compares closely to the standard dose of 1500 mg/d for patients.

As expected from the minimal human toxicity, there was no significant difference in the weights between the vehicle- and atovaquone-treated animals. Importantly, treatment with either pure atovaquone or Mepron significantly reduced tumor growth and extended survival compared with vehicle (Figure 4). Thus, atovaquone shows evidence of anticancer activity in vivo.

Atovaquone is active against primary leukemic cells and in serum of treated patients

To extend these findings beyond hematological cancer cell lines, we obtained primary leukemic blasts from patients with AML or ALL, both of which demonstrate STAT3 activation with high frequency.²⁴ Atovaquone inhibited STAT3 tyrosine phosphorylation in these primary cancer cells both at baseline and following exposure to IL-6, as may occur in the bone marrow microenvironment (Figure 5A; supplemental Figure 3A). Additionally, atovaquone decreased the expression of multiple key STAT3 target genes in the leukemic cells and markedly reduced their viable cell number (Figure 5B; supplemental Figure 3B-C).

Clinically, atovaquone is frequently used to prevent *P. jirovecii* pneumonia in hematological cancer patients after allogeneic HSCT. At the Dana-Farber/Brigham and Women's Cancer Center, HSCT patients are prescribed atovaquone in the first 20 to 30 days after transplant, and then switched to long-term treatment with another anti-*Pneumocystis* antibiotic, trimethoprim-sulfamethoxazole (Bactrim), once stable engraftment has occurred. However, a substantial minority of patients are instead maintained on atovaquone for months to years because of allergy to or intolerance of trimethoprim-sulfamethoxazole.

To analyze whether atovaquone administered to patients could exhibit anticancer activity, we incubated U266 multiple myeloma cells with serum collected from patients ~100 days following HSCT who were receiving either trimethoprim-sulfamethoxazole or atovaquone for *Pneumocystis* prophylaxis. The samples from patients taking atovaquone were distinguished by a darker, redder hue (Figure 1C), reflecting the visible presence of drug in the patients' circulation. Exposure to serum from atovaquone-treated patients led to reduced viable cell number of U266 cells compared with exposure to serum of patients receiving trimethoprim-sulfamethoxazole (supplemental Figure 3D), suggesting that the presence of atovaquone in patient sera exerts anticancer activity.

Atovaquone administration is associated with improved outcomes in cancer patients

Because of the requirement for *Pneumocystis* prophylaxis post-HSCT, a large proportion of these patients receive long-term atovaquone treatment. This provided a unique opportunity to investigate the anticancer effects of atovaquone in patients through a retrospective analysis of the relationship between duration of atovaquone treatment and clinical outcomes after HSCT. To analyze a uniform population, we focused on AML patients who underwent allogeneic HSCT with myeloablative conditioning between 2005 and 2012 at the Dana-Farber/Brigham and Women's Cancer Center. This group was chosen for its large sample size, the efficacy of atovaquone against AML cell lines in vitro (eg, HEL) and primary AML blasts, and frequent STAT3 activation in AML patient samples.²⁴ The analysis comprised patients

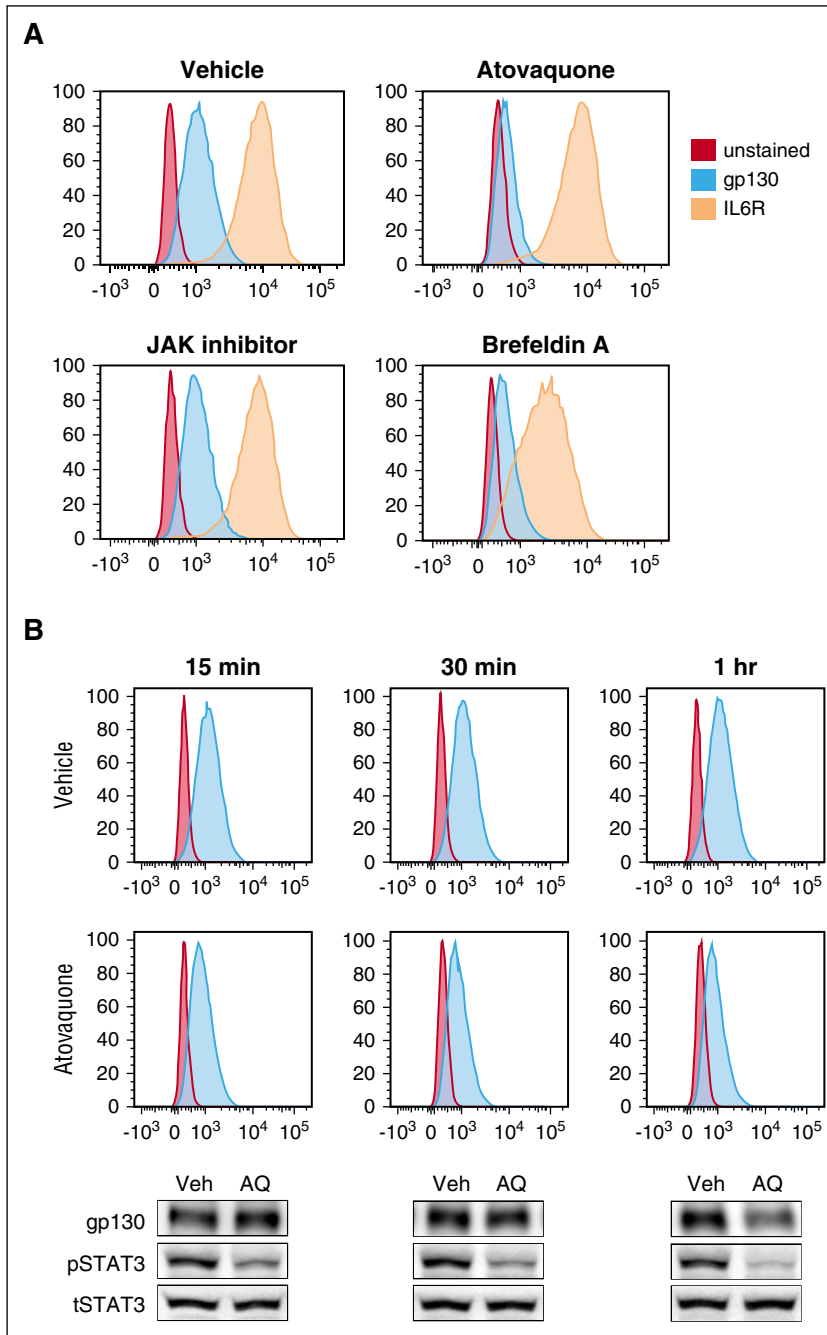


Figure 3. Atovaquone specifically and rapidly down-regulates cell-surface expression of gp130. (A) U266 cells were treated with atovaquone (20 μ M), JAK inhibitor 1 (1 μ M), or brefeldin A (3 μ g/mL) for 2.5 hours, then analyzed by flow cytometry for cell-surface expression of gp130 and IL-6 receptor (CD126). Data are representative of 3 independent experiments. (B) U266 cells were treated with atovaquone at 20 μ M for the indicated time periods, and then cells were assayed by western blot or flow cytometry from the same experimental treatment. Data are representative of 2 independent experiments.

who survived relapse-free at least 150 days after HSCT because of the increased rate of nonrelapse mortality in the immediate posttransplant period, to allow for accrual of time on atovaquone treatment, and to avoid a guarantee-time bias.

Among this patient population, initial *Pneumocystis* prophylaxis consists of atovaquone beginning at discharge from hospitalization. Patients who do not have an allergy to Bactrim are switched to this drug once their blood counts have stabilized. This treatment approach is independent of conditioning regimen or prophylactic regimen for GVHD. Because nearly all patients receive atovaquone for at least 20 days after HSCT, patients receiving atovaquone for 55 days or more within the first 150 days were categorized as “high atovaquone” exposure (N = 96), whereas the remainder were classified as “low atovaquone” exposure (N = 136).

The cutoff of 55 days was selected based on a statistical analysis (delineated in Methods), and it also corresponds to the tail of the primary peak of atovaquone treatment duration. The clinical characteristics of both groups are summarized in supplemental Table 4. Notably, patients in the “high atovaquone” group had a lower rate of relapse of AML compared with those in the “low atovaquone” group (3-year cumulative incidence of relapse: 13% vs 23%, $P = .037$; Figure 5C), with no difference in nonrelapse mortality ($P = .77$). This result was consistent in multivariable analysis. In multivariable analysis on cumulative incidence of relapse adjusting for the variables listed in supplemental Table 4 and the occurrence of grade 2 to 4 acute GVHD, the subdistribution hazard ratio for “high atovaquone” exposure was 0.49 (95% CI, 0.25-0.96; $P = .039$).

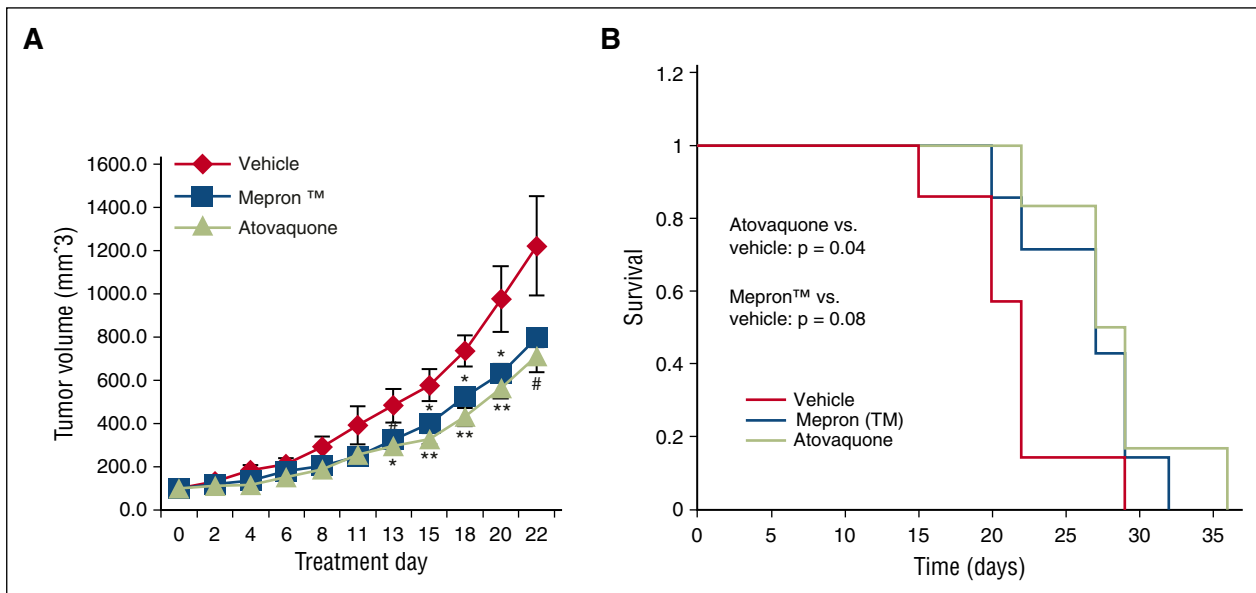


Figure 4. Atovaquone demonstrates in vivo antitumor activity in a murine model of multiple myeloma. (A) Following establishment of U266 tumor xenografts, mice were treated orally with vehicle (N = 7), atovaquone (N = 6), or brand-name Mepron suspension (N = 7). Tumor volume was assessed 3 times per week. Data are means \pm standard error, and *P* values represent comparisons of atovaquone and Mepron to vehicle by 2-tailed Wilcoxon rank-sum test. #*P* < .10; **P* < .05; ***P* < .01. (B) Kaplan-Meier survival plot of the mice described for panel A. *P* values comparing atovaquone or Mepron survival curves to that of vehicle were computed by 2-tailed log-rank test.

Discussion

We discovered atovaquone, an FDA-approved antimicrobial drug not previously known to have any effects in mammalian cells, as a novel STAT3 inhibitor using an unbiased gene expression–based approach. Atovaquone uniquely acts by diminishing gp130 expression at the cell surface, thus decreasing the availability of a key protein involved in STAT3 activation. As a result, atovaquone causes substantial inhibition of STAT3 tyrosine phosphorylation and transcriptional activity. Consequently, the expression of critical STAT3 target genes mediating survival and proliferation is reduced, including survivin, Bcl-2 family members, and cyclin D1. Atovaquone decreases the viability of STAT3-dependent cancer cells by apoptosis at concentrations routinely achieved with standard clinical doses.

Atovaquone inhibition of STAT3 signaling from IL-6, which requires gp130, may have broad therapeutic implications because this is a key oncogenic pathway across diverse tumor types.^{25–27} For example, IL-6 is a critical survival factor in AML and multiple myeloma,^{27,28} which is reflected in the activity of atovaquone on the cell lines used here and our findings in the animal model and in AML patients. The importance of IL-6 has been established in multiple solid malignancies as well, including breast, lung, and melanoma.^{29,30} In addition to inhibiting IL-6, we showed that atovaquone also inhibits signaling from OSM, which is another cytokine that utilizes gp130. This is advantageous because OSM also activates STAT3, resulting in oncogenic effects.^{31–33} Moreover, by downregulating cell-surface gp130, atovaquone inhibits the overactive mutant JAK2-V617F, whose critical role in hematological malignancies is well recognized.³⁴ On the other hand, 1 mechanism of resistance to kinase inhibitors is the subversion of a parallel pathway to lead to comparable activation of STATs (or other transcription factors). Although we have not yet been able to derive cells resistant to the cytotoxic effects of atovaquone, it is conceivable that activation of STAT3 through a non-gp130-dependent pathway would be 1 mechanism by which the effect of atovaquone could be evaded.

It is not known currently how atovaquone induces downregulation of gp130, independent of other physically associated proteins. It has been suggested that compounds that can induce the phosphorylation of gp130 on serine-782 can lead to a downregulation of glycosylation of gp130 and destabilization of the protein.²¹ Although atovaquone does not appear to be acting through this exact mechanism, it does raise the possibility that membrane trafficking of gp130 can be modulated specifically.

Atovaquone is more selective than direct pharmacological JAK inhibition because the effects of atovaquone are restricted to gp130-dependent processes. For example, atovaquone did not affect the signaling of interferon- γ , which activates STAT1, or prolactin, which activates STAT5 (Figure 1E). Interferon and prolactin cause JAK-dependent STAT activation, but they do not use gp130; therefore, their activities are blocked by JAK inhibitors but remain intact with atovaquone treatment. Additionally, numerous other factors require JAKs but not gp130, including leptin, growth hormone, and erythropoietin. Atovaquone is known to be extremely well tolerated in humans, and this may reflect its selectivity for gp130-dependent signaling compared with therapies that target JAK signaling more broadly. The direct molecular target or targets of atovaquone in mammalian cells are not known at this time. Atovaquone is known to bind to mitochondrial cytochrome bc₁ complex in parasites.³⁵ Although the affinity of atovaquone for this complex is much lower in mammalian cells, it is possible that at the high concentrations achieved in humans, this cytochrome is bound by the drug in these hematopoietic cells. Nonetheless, this study has laid the groundwork for future research that may lead to the elucidation of its mechanism in inhibiting gp130, thus potentially uncovering important new cellular targets for cancer drug discovery efforts.

Importantly, multiple lines of evidence from our work support the translational potential of atovaquone as an anticancer therapy in humans. First, atovaquone is a well-tolerated, FDA-approved medication, and all of our studies used drug concentrations routinely achieved in patients. Second, oral administration of atovaquone to mice decreased tumor growth and prolonged survival. Third, atovaquone

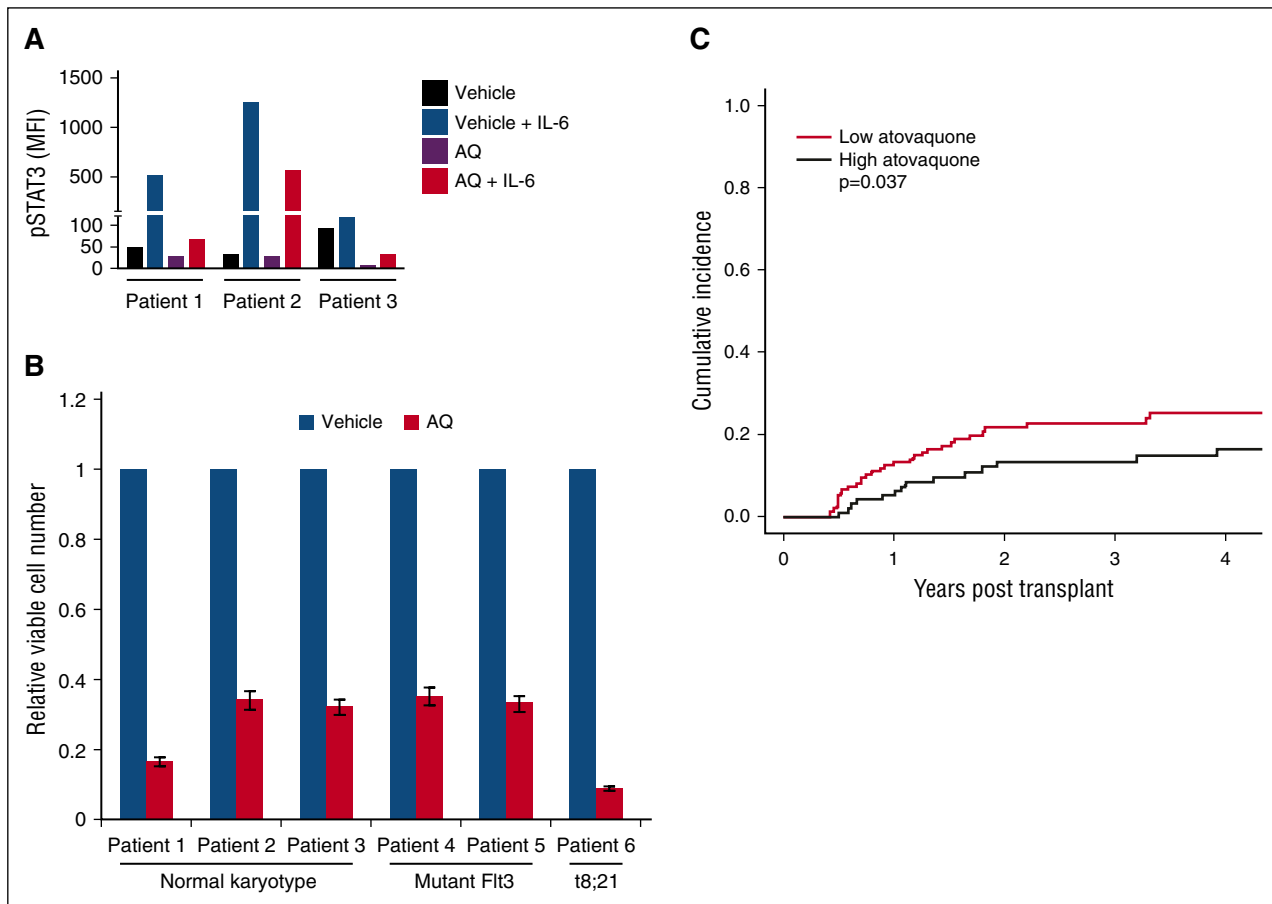


Figure 5. Atovaquone demonstrates evidence of anticancer efficacy against primary leukemic blasts and in patients with AML. (A) Primary leukemic blasts from 3 AML patients were obtained, pretreated with vehicle or atovaquone (25 μ M) for 16 hours, and then treated with IL-6 (50 ng/mL) for 15 minutes followed by flow cytometric assessment of STAT3 phosphorylation. MFI, mean fluorescence intensity. Data are representative of 2 independent experiments. (B) The primary cancer cells described in panel A were treated with vehicle or atovaquone (25 μ M) for 72 hours, after which viable cell number was assessed. Data are means \pm standard deviation of 2 independent experiments. (C) Cumulative incidence of relapse of patients with AML following allogeneic HSCT (see text), classified as >55 days of atovaquone treatment within the first 150 days posttransplant ("high atovaquone") or otherwise ("low atovaquone"). *P* value is 2-tailed using Gray's test.

treatment of primary, patient-derived AML and ALL cells inhibited STAT3 and decreased their viability. Fourth, serum of patients taking atovaquone inhibited growth of cancer cells. Fifth, retrospective analysis of AML patients after HSCT revealed improved relapse-free survival with greater atovaquone exposure.

One limitation of the clinical study is its retrospective nature. However, a priori, it may be predicted that AML patients in the "high atovaquone" group would actually have worse outcomes. First, atovaquone is less effective than trimethoprim-sulfamethoxazole in treating *Pneumocystis pneumonia*, a potentially life-threatening infection.³⁶ Second, patients are often switched from trimethoprim-sulfamethoxazole back to atovaquone or maintained continuously on atovaquone because of persistently low blood counts, which often reflects poor graft function and may portend relapse of the underlying AML. Thus, it is notable that atovaquone was associated with an improved cancer outcome in this cohort. Because atovaquone can inhibit IL-6–mediated activation of STAT3 in nonneoplastic cells, it is possible that a beneficial effect of atovaquone in this population was mediated by an effect distinct from the direct antileukemic effects seen in vitro, such as decreased inflammation or an enhanced immune response. Further studies will be important to clarify this point.

AML is a disease with a 5-year survival rate of only 20% to 40%, and the mainstay of treatment, cytotoxic chemotherapy, has remained unchanged for decades.³⁷ Our data, taken together, demonstrate

atovaquone to be an effective STAT3 inhibitor with evidence of anticancer activity in both animal models and in patients, for AML and for other hematological malignancies. Additionally, its FDA-approved status ensures it is clinically available and ideally poised to be repurposed as a treatment of cancer. With the pressing need to develop therapeutic approaches targeting novel molecular pathways, as well as the absence of STAT3 inhibitors in the clinic, it would be useful to evaluate the anticancer efficacy of atovaquone in a prospective clinical trial.

Acknowledgments

This work was supported by the National Cancer Institute, National Institutes of Health (grant R01-CA160979); When Everyone Survives Foundation (Duluth, GA); Gabrielle's Angel Foundation (New York, NY); Lymphoma Research Foundation (New York, NY); the DeGregorio Family Foundation (Pleasantville, NY); the Kittredge Foundation; the Brent Leahey Fund (D.A.F.); the National Institute of General Medical Sciences (grants T32GM007753 and F30 CA165740-01) (M.X.); and Millennium Nucleus-P-07-011-F and FONDAP-15150012 (C.H.). This research was also supported by a generous gift from Stephen P. Koster.

Authorship

Contribution: M.X. designed and performed experiments, analyzed data, and wrote the manuscript; H.K. and V.T.H. provided access to clinical records and performed statistical analyses; S.R.W., M.B.-N., M.A., S.L., P.A.T., Y.K., N.J., Z.T.G., L.N.H., D.Q.Y., J.J.M., and D.S. performed experiments and analyzed data; J.E.B., T.B., D.N., C.H., R.M.S., and R.J.S. designed experiments and analyzed data;

and D.A.F. designed experiments, analyzed data, and provided editorial input.

Conflict-of-interest disclosure: The authors declare no competing financial interests.

The current affiliation for M.X. is Department of Radiation Oncology, Stanford School of Medicine, Stanford, CA.

Correspondence: David A. Frank, Dana-Farber Cancer Institute, 450 Brookline Ave, Boston, MA 02215; e-mail: david_frank@dfci.harvard.edu.

References

- Sawyers C. Targeted cancer therapy. *Nature*. 2004;432(7015):294-297.
- Frank DA. Transcription factor STAT3 as a prognostic marker and therapeutic target in cancer. *J Clin Oncol*. 2013;31(36):4560-4561.
- Xiang M, Birkbak NJ, Vafaizadeh V, et al. STAT3 induction of miR-146b forms a feedback loop to inhibit the NF- κ B to IL-6 signaling axis and STAT3-driven cancer phenotypes. *Sci Signal*. 2014;7(310):ra11.
- Nelson EA, Walker SR, Kepich A, et al. Nifuroxazide inhibits survival of multiple myeloma cells by directly inhibiting STAT3. *Blood*. 2008;112(13):5095-5102.
- Frank DA. STAT3 as a central mediator of neoplastic cellular transformation. *Cancer Lett*. 2007;251(2):199-210.
- O'Shea JJ, Holland SM, Staudt LM. JAKs and STATs in immunity, immunodeficiency, and cancer. *N Engl J Med*. 2013;368(2):161-170.
- Haftchenary S, Avadisian M, Gunning PT. Inhibiting aberrant Stat3 function with molecular therapeutics: a progress report. *Anticancer Drugs*. 2011;22(2):115-127.
- Lamb J, Crawford ED, Peck D, et al. The Connectivity Map: using gene-expression signatures to connect small molecules, genes, and disease. *Science*. 2006;313(5795):1929-1935.
- Hieronymus H, Lamb J, Ross KN, et al. Gene expression signature-based chemical genomic prediction identifies a novel class of HSP90 pathway modulators. *Cancer Cell*. 2006;10(4):321-330.
- Wei G, Twomey D, Lamb J, et al. Gene expression-based chemical genomics identifies rapamycin as a modulator of MCL1 and glucocorticoid resistance. *Cancer Cell*. 2006;10(4):331-342.
- Alvarez JV, Febbo PG, Ramaswamy S, Loda M, Richardson A, Frank DA. Identification of a genetic signature of activated signal transducer and activator of transcription 3 in human tumors. *Cancer Res*. 2005;65(12):5054-5062.
- Walker SR, Nelson EA, Frank DA. STAT5 represses BCL6 expression by binding to a regulatory region frequently mutated in lymphomas. *Oncogene*. 2007;26(2):224-233.
- Battle TE, Arbiser J, Frank DA. The natural product honokiol induces caspase-dependent apoptosis in B-cell chronic lymphocytic leukemia (B-CLL) cells. *Blood*. 2005;106(2):690-697.
- Frank DA, Mahajan S, Ritz J. B lymphocytes from patients with chronic lymphocytic leukemia contain signal transducer and activator of transcription (STAT) 1 and STAT3 constitutively phosphorylated on serine residues. *J Clin Invest*. 1997;100(12):3140-3148.
- Gray RJ. A class of K-sample tests for comparing the cumulative incidence of a competing risk. *Ann Stat*. 1988;16(3):1141-1154.
- Fine JP, Gray RJ. A proportional hazards model for the subdistribution of a competing risk. *J Am Stat Assoc*. 1999;94(446):496-509.
- Harrell FE Jr. Regression Modeling Strategies: With Applications to Linear Models, Logistic Regression, and Survival Analysis. New York: Springer-Verlag; 2001.
- Baggish AL, Hill DR. Antiparasitic agent atovaquone. *Antimicrob Agents Chemother*. 2002;46(5):1163-1173.
- Burger R, Le Gouill S, Tai YT, et al. Janus kinase inhibitor INCB20 has antiproliferative and apoptotic effects on human myeloma cells in vitro and in vivo. *Mol Cancer Ther*. 2009;8(1):26-35.
- Lu X, Levine R, Tong W, et al. Expression of a homodimeric type I cytokine receptor is required for JAK2V617F-mediated transformation. *Proc Natl Acad Sci USA*. 2005;102(52):18962-18967.
- Andraos R, Qian Z, Bonenfant D, et al. Modulation of activation-loop phosphorylation by JAK inhibitors is binding mode dependent. *Cancer Discov*. 2012;2(6):512-523.
- Comley JC, Sterling AM. Effect of atovaquone and atovaquone drug combinations on prophylaxis of *Pneumocystis carinii* pneumonia in SCID mice. *Antimicrob Agents Chemother*. 1995;39(4):806-811.
- Reagan-Shaw S, Nihal M, Ahmad N. Dose translation from animal to human studies revisited. *FASEB J*. 2008;22(3):659-661.
- Lin TS, Mahajan S, Frank DA. STAT signaling in the pathogenesis and treatment of leukemias. *Oncogene*. 2000;19(21):2496-2504.
- Hedvat M, Huszar D, Herrmann A, et al. The JAK2 inhibitor AZD1480 potentially blocks Stat3 signaling and oncogenesis in solid tumors. *Cancer Cell*. 2009;16(6):487-497.
- Reynaud D, Pietras E, Barry-Holson K, et al. IL-6 controls leukemic multipotent progenitor cell fate and contributes to chronic myelogenous leukemia development. *Cancer Cell*. 2011;20(5):661-673.
- Schuringa JJ, Wierenga AT, Kruijer W, Vellenga E. Constitutive Stat3, Tyr705, and Ser727 phosphorylation in acute myeloid leukemia cells caused by the autocrine secretion of interleukin-6. *Blood*. 2000;95(12):3765-3770.
- Klein B, Zhang XG, Lu ZY, Bataille R. Interleukin-6 in human multiple myeloma. *Blood*. 1995;85(4):863-872.
- Hoejberg L, Bastholt L, Schmidt H. Interleukin-6 and melanoma. *Melanoma Res*. 2012;22(5):327-333.
- Schafer ZT, Brugge JS. IL-6 involvement in epithelial cancers. *J Clin Invest*. 2007;117(12):3660-3663.
- Fossey SL, Bear MD, Kisseberth WC, Pennell M, London CA. Oncostatin M promotes STAT3 activation, VEGF production, and invasion in osteosarcoma cell lines. *BMC Cancer*. 2011;11:125.
- Li Q, Zhu J, Sun F, Liu L, Liu X, Yue Y. Oncostatin M promotes proliferation of ovarian cancer cells through signal transducer and activator of transcription 3. *Int J Mol Med*. 2011;28(1):101-108.
- West NR, Murray JI, Watson PH. Oncostatin-M promotes phenotypic changes associated with mesenchymal and stem cell-like differentiation in breast cancer. *Oncogene*. 2014;33(12):1485-1494.
- Kiladjian JJ. The spectrum of JAK2-positive myeloproliferative neoplasms. *Hematology Am Soc Hematol Educ Program*. 2012;2012:561-566.
- Birth D, Kao W-C, Hunte C. Structural analysis of atovaquone-inhibited cytochrome bc1 complex reveals the molecular basis of antimalarial drug action. *Nat Commun*. 2014;5:4029.
- Hughes W, Leoung G, Kramer F, et al. Comparison of atovaquone (566C80) with trimethoprim-sulfamethoxazole to treat *Pneumocystis carinii* pneumonia in patients with AIDS. *N Engl J Med*. 1993;328(21):1521-1527.
- Nelson EA, Walker SR, Xiang M, et al. The STAT5 inhibitor pimozide displays efficacy in models of acute myelogenous leukemia driven by FLT3 mutations. *Genes Cancer*. 2012;3(7-8):503-511.